*CHEESA: Chemical Engineering Research Articles*
ISSN 2614-8757 (Print), ISSN 2615-2347 (Online)
Homepage: https://e-journal.unipma.ac.id/index.php/cheesa

Research Article

OPEN ACCESS

CHEESA, 9(1), pp 41-52, 2026

# Hybrid Paper Membrane Based on Abaca (*Musa textilis*) Fibers and Rice Husk Ash Silica Using Citric Acid as a Cross-Linking Agent for the Removal of Dyes and Heavy Metals

**Ian Kurniawan[1*)], Adri Huda[2)], Reisya Ichwani[3)], Dina Nasution[4)], Nasrul Rofiah Hidayati[5)], Noor Haida Mohd Kaus[6)]**

[1)]*Universitas PGRI Palembang, Department of Chemical Engineering, Faculty of Engineering and Informatics, Jl. Ahmad Yani,Palembang 30166, Indonesia*

[2)]*Universitas Sumatera Utara, Department of Environmental Engineering, Faculty of Engineering, Jalan Almamater Kampus USU Padang Bulan, Medan 20155, Indonesia*

[3)]*Universitas Sumatera Utara, Department of Mechanical Engineering, Faculty of Engineering, Medan 20155, Indonesia*

[4)]*Universitas Negeri Padang, Department of Chemistry, Faculty of Mathematics and Natural Sciences, Jalan Prof. Dr. Hamka, Air Tawar, Padang 25131, Indonesia*

[5)]*Universitas PGRI Madiun, Departement of Chemical Engineering, Faculty of Engineering, Jl. Setia Budi, Madiun 63118, Indonesia*

[6)]*Universiti Sains Malaysia, School of Chemical Science, Pulau Penang 11800, Malaysia*

*corresponding author: iankurniawan@univpgri-palembang.ac.id

**Article History**

*Submitted: 16th February 2026; Revised: 14th August 2026; Accepted: 15th August 2026;*

*Available online: 26th August 2026; Published Regularly: June 2026*

**doi**: 10.25273/cheesa.v9i1.24288.41-52

## Abstract

The pollution from wastewater containing synthetic dyes and heavy metals is a serious environmental issue in Indonesia. The situation is associated with the lack of locally sourced membranes to simultaneously integrate physical filtration and chemical adsorption mechanisms (filtro-adsorption). Therefore, this research aims to develop a hybrid paper membrane based on abaca (*Musa textilis*) fiber pulp and rice husk ash silica using citric acid as a cross-linking agent for the removal of methylene blue (MB) dye and heavy metal ions ($Cu^{2+}$ and $Pb^{2+}$) from synthetic wastewater. The methodology required silica extraction from rice husk ash through an alkaline method and modification of the product with 3-aminopropyltriethoxysilane (APTES)s. There was also membrane fabrication with different variations of silica (0–20% of dry fiber weight) and citric acid (0–15%) contents, as well as characterization through X-ray Diffraction (XRD), Fourier Transform Infrared Spectroscopy (FTIR), and Scanning Electron Microscopy with Energy Dispersive X-ray Spectroscopy (SEM-EDS). The results showed that the optimal membrane with 15% silica and 10% citric acid achieved a water flux of 285 L/m²·h·bar and removal efficiencies of >95% for MB ($C_0$ = 50 mg/L), 78.5 ± 3.2% for $Cu^{2+}$, and 82.3 ± 2.8% for $Pb^{2+}$ ($C_0$ = 10 mg/L). The two-way analysis of variance (ANOVA) also confirmed that the variations in silica and citric acid content significantly affected the separation performance ($p < 0.05$). The results showed that the hybrid membrane derived from abundant local agricultural waste had potential as an environmentally friendly wastewater treatment technology.

**Keywords:** citric acid; cross-linking; hybrid membrane; rice husk ash silica; wastewater separation

## 1. Introduction

The pollution from wastewater containing synthetic dyes and heavy metals is an environmental issue that continues to escalate with the growth of the textile, batik, leather tanning, and metal plating industries in Indonesia. The condition is associated with the fact that cationic dyes such as methylene blue (MB) are persistent and difficult to degrade [1],[2],[3] while heavy metal ions in the form of $Cu^{2+}$ and $Pb^{2+}$ are non-biodegradable and highly toxic to aquatic ecosystems and human health [4]. A 2024 report by the Indonesian Ministry of Environment and Forestry (KLHK) showed that industrial waste contributed approximately 45% to the total national

This is an open access article under the CC BY license (http://creativecommons.org/licenses/by/4.0/)

water pollution load and reflected the need for the development of effective, affordable, and environmentally friendly treatment technologies [5].

Several conventional technologies have been adopted to treat industrial wastewater including coagulation-flocculation [6], activated carbon adsorption [1], ion exchange [1], and chemical oxidation [5]. However, each has limitations with coagulation-flocculation generating large volumes of sludge [7] and activated carbon adsorption requiring high operating costs [1]. Synthetic polymer-based membrane technologies such as nanofiltration and reverse osmosis are also highly effective but require high production costs, prone to fouling, and less environmentally friendly [2],[4],[8]. These limitations motivate the need to develop sustainable membranes based on local materials [2],[9],[10].

Hybrid membrane technology which simultaneously combines physical filtration and chemical adsorption mechanisms such as filtro-adsorption within a single material offers a promising alternative. Cellulose-based natural fibers are considered to have significant potential as membrane matrices in this context due to their renewable and biodegradable nature, inherent hydrophilicity, and low cost [1]. However, pure cellulose membranes have poor mechanical stability under wet conditions which leads to the need for modification [4].

Indonesia has significant potential to utilize agricultural waste such as rice husks. The ash of rice husks after calcination contains amorphous silica characterized by a high surface area, a mesoporous structure, and active silanol (Si–OH) groups that facilitate pollutant adsorption mechanisms [8]. The incorporation of silica into the cellulose membrane matrix enhances mechanical strength and increases adsorption capacity for cationic dyes and heavy metal ions [2].

Citric acid is an environmentally friendly and non-toxic cross-linking agent that forms ester bonds with cellulose hydroxyl groups via esterification at moderate temperatures. It has been used to improve the wet strength and dimensional stability of membranes without compromising biodegradability and in line with green chemistry principles [3].

Previous research has reported the use of rice husk ash silica in synthetic polymer and chitosan membrane systems. Astuti & Susilowati [1] reported enhanced hydrophilicity in polysulfone/chitosan membranes after the addition of rice husk ash silica. Malafatti et al [11] also developed silica-modified polylactic acid membranes for dye removal and Hubadillah et al [12] successfully applied hollow-fiber ceramic membranes from rice husk ash for heavy metal removal with an efficiency of >80%. However, very limited research specifically combines abaca (*Musa textilis*) fibers from South Sumatra as a paper membrane matrix, rice husk ash silica as a functional reinforcement, and citric acid as the cross-linking agent in a single hybrid filter-adsorption membrane system for the simultaneous removal of dyes and heavy metals. The novelty of this research is the integration of the three components using abundant local raw materials [13].

The aim is to develop a hybrid paper membrane based on abaca fibers from Ogan Ilir, South Sumatra, and rice husk ash silica cross-linked with citric acid, characterize the structure and morphology of the membrane using X-ray Diffraction (XRD), Fourier Transform Infrared Spectroscopy (FTIR), and Scanning Electron Microscopy with Energy Dispersive X-ray Spectroscopy (SEM-EDS), as well as evaluate its performance in removing MB dye and heavy metals ($Cu^{2+}$ and $Pb^{2+}$) from synthetic wastewater. The developed membrane is expected to serve as an environmentally friendly and low-cost wastewater treatment solution based on local resources available in Indonesia.

## 2. Research Methods

An experimental design with two factors was adopted including variations in rice husk ash silica content at 0%, 5%, 10%, 15%, and 20% by dry fiber weight with the citric acid concentration as a cross-linking agent at 0%, 5%, 10%, and 15% by dry fiber weight. A control membrane produced with 0% silica and 0% citric acid was coded M0 and included to show the effect of each component. Each variation was tested in triplicate and coded as M0 through M7. These included M1–M4 for the variations of the silica content at 5%, 10%, 15%, and 20% without citric acid. M5–M7 maintained a constant silica content of 15% with varying citric acid concentrations at 5%, 10%, and 15%. The potential for membrane reuse was evaluated by applying a regeneration test on the optimal membrane (M6) over three consecutive cycles. The filtration process was followed by the immersion of the membrane in a 0.1 M $HNO_3$ solution for 30 minutes to desorb heavy metal ions and MB and rinsed with distilled water until a neutral pH was achieved.

2.1 Tools and Materials

The primary materials used were abaca fibers obtained in a postharvest-dried state from a plantation in Ogan Ilir Regency, South Sumatra and the Ciherang-variety rice husks from a rice mill in Banyuasin Regency, South Sumatra. The chemicals used were sodium hydroxide (NaOH, ≥99%), hydrochloric acid (HCl, 37%, analytical grade), 3-aminopropyltriethoxysilane (APTES, ≥98%), citric acid monohydrate (≥99.5%), distilled water (TDS < 5 ppm), and deionized water produced using a Barnstead Smart2Pure system, Thermo Scientific.

Synthetic wastewater was prepared to evaluate membrane performance. This was achieved using the test solutions consisting of MB (MB, ≥82%) at an initial concentration ($C_0$) of 50 mg/L as a model cationic dye with $CuSO_4 \cdot 5H_2O$ (≥99%) and $Pb(NO_3)_2$ (≥99%) each at $C_0$ = 10 mg/L as model heavy metal ions ($Cu^{2+}$ and $Pb^{2+}$). All the test solutions were prepared using distilled water.

The equipment used was categorized into general and characterization types. The general equipment included an analytical balance, a hot plate magnetic stirrer, a mechanical pulp refiner, a drying oven, a vacuum filtration unit, a membrane mold (5 cm diameter, 19.6 cm² effective area), and a pH meter. Meanwhile, the characterization equipment consisted of a digital micrometer for measuring membrane thickness, a Universal Testing Machine (UTM) for mechanical stability tests in line with the ASTM D882 standard, an X-ray diffractometer with a Cu-Kα source (λ = 1.5406 Å), a 2θ range of 5–80°, and a scanning speed of 2°/min. It also included FTIR in the 400–4000 $cm^{-1}$ range using KBr pellets, SEM operated at 10 kV with magnifications of 1,000×, 5,000×, and 20,000×, a UV–Vis spectrophotometer, and an Atomic Absorption Spectrophotometer.

2.2 Silica Extraction from Rice Husk Ash

Silica was extracted from rice husk ash which was considered an abundant agricultural waste product. The extraction procedure was initiated with the washing of the rice husks followed by oven-drying at 105°C for 24 hours. The dried husks were calcined in a muffle furnace at 700°C for 3 hours at a heating rate of 10°C/min to produce white ash with $SiO_2$ content of ≥ 95% [14]. Subsequently, 10 g of rice husk ash was extracted using 100 mL of 1 M NaOH solution at 80°C for 1 hour under stirring at 300 rpm to form sodium silicate ($Na_2SiO_3$).

Filtration was conducted and the $Na_2SiO_3$ solution was acidified by adding 2 M HCl dropwise up to the achievement of pH 7 which led to the precipitation of amorphous silica. The precipitate was filtered, washed with distilled water to remove chlorides, and dried at 110°C for 12 hours. Surface modification of the silica was conducted by dispersing 5 g of dried silica into 100 mL of absolute ethanol with the addition of 5% (v/v) APTES and stirring the mixture at 60°C for 6 hours. The silica-APTES product was filtered, washed with ethanol, and dried at 80°C for 4 hours.

2.3 Hybrid Paper Membrane Fabrication

The abaca fibers were processed into pulp by soaking in a 4% NaOH solution at 80°C for 4 hours to delignify, rinsing to achieve neutrality, and refining with a mechanical pulp refiner for the purpose of obtaining a homogeneous fiber suspension (1% w/v consistency). The selection of silica composition variations of 0–20% was based on preliminary research to identify the optimal balance between mechanical properties and separation performance.

Modified rice husk ash silica was added to the fiber suspension according to the composition variations and stirred with a magnetic stirrer for 30 minutes at 25 ± 2°C to achieve a homogeneous mixture. Citric acid was subsequently added at varying concentrations of 0–15% and stirred for 15 minutes. The suspension was formed into sheets using a vacuum filtration method (–0.7 bar) in a mold with a 5 cm diameter at an effective area of 19.6 cm². The wet membrane was dried in an oven at 80°C for 2 hours to activate the esterification or cross-linking reaction. Moreover, the dry membrane thickness of 150–200 µm was verified using a digital micrometer and conditioned in a desiccator at 25 ± 2°C for 24 hours before tests were conducted.

2.4 Membrane Characterization

The thickness was measured using a digital micrometer at five different points and the values recorded were averaged. Water absorption was measured gravimetrically in line with ASTM D570 (SNI 06-4822-1998) and mechanical stability was tested using a UTM based on ASTM D882. The evidence of ester cross-linking formation was confirmed by FTIR peak shifts with a specific focus on the appearance of a new peak at ~1730 $cm^{-1}$ (ester C=O) and a decrease in O–H intensity (~3300 $cm^{-1}$) in the citric acid-treated membrane compared to the control [15]. Meanwhile, the presence of silica was confirmed through EDS analysis and SEM observations.

2.5 Membrane Performance Test

Separation performance was determined using the dead-end filtration method at a pressure of 1 bar which was the standard for laboratory-scale microfiltration–ultrafiltration membrane test and a temperature of 25 ± 2°C. Meanwhile, the water flux was calculated using the following Equation 1. J was the flux (L/m²·h), V was the permeate volume (L), A was the effective surface area (m²), and t was the filtration time (h).

$$J = \frac{V}{A \times t} \quad \text{.....(Equation 1)}$$

MB concentration was determined through three stages of UV–Vis spectrophotometric measurement. These included the (1) evaluation of the maximum wavelength (λmax) by scanning a single concentration of MB standard solution across the 400–800 nm range, (2) construction of a standard calibration curve by measuring absorbance at λmax against a series of MB standard solution concentrations, and (3) the measurement of feed and permeate solution absorbance at the same λmax, followed by conversion to concentration (mg/L) using the calibration curve equation. The application of stage (1) led to the determination of λmax as 664 nm. Heavy metal concentrations were analyzed using AAS at λ = 324.8 nm for Cu and λ = 217.0 nm for Pb. Meanwhile, removal efficiency was calculated using the following Equation 2. $C_0$ was the initial feed solution concentration (mg/L) and $C_p$ was the concentration in the permeate (mg/L).

$$R\ (\%) = \frac{C_0 - C_p}{C_0} \times 100\% \quad \text{.....(Equation 2)}$$

2.6 Statistical Analysis

Data were analyzed using two-way analysis of variance (ANOVA) at the 95% confidence level (α = 0.05) in SPSS 25.0 to evaluate the effects of silica content, citric acid concentration, and the interaction between the two. A Tukey's Honest Significant Difference (HSD) post-hoc test was also performed in situations where $p < 0.05$. The results are presented with error bars representing the standard deviation of three replicates [6],[7].

## 3. Results and Discussion

3.1. Separation Performance for Methylene Blue Dye and Heavy Metals $Cu^{2+}$ and $Pb^{2+}$

The mechanical properties of the membrane were characterized to ensure structural integrity during filtration before the pollutant-removal capability was evaluated. Table 1 presents the mechanical properties with a focus on the thickness, tensile strength, and strain of all hybrid paper membrane variations. Table 1 shows that the addition of silica and citric acid increased the thickness and tensile strength but reduced the strain of the membrane variations. Membrane M6 (15% silica, 10% citric acid) recorded the highest tensile strength of 22.3 MPa and a thickness of 185 µm which signaled the existence of optimal cross-linking. This enhancement in mechanical strength was expected to support membrane stability during the filtration process. Meanwhile, an increase in the silica and citric acid content tended to reduce water flux due to the improvement of the membrane density and significantly enhanced the removal efficiency for MB, $Cu^{2+}$, and $Pb^{2+}$. M6 showed the best performance by achieving removal efficiencies of >95% for MB, 78.5% for $Cu^{2+}$, and 82.3% for $Pb^{2+}$ which led to its confirmation as the optimal variation. The reduction in MB concentration listed in Table 1 was visualized through a UV-Vis spectrophotometric analysis.

Figure 1 presents the absorption spectra of the MB solution before and after filtration using the control M0 and the optimal membrane M6. The spectra were recorded in the 400–800 nm wavelength range, with the maximum absorption peak (λmax) for MB observed at 664 nm. A highly significant decrease was recorded in the absorbance of M6 at λ = 664 nm after filtration compared to M0. M6 also achieved a MB removal efficiency of >95% while M0 recorded only 61.2 ± 2.8%. The two-way ANOVA results also confirmed that the difference was statistically significant ($p < 0.05$).

This enhanced efficiency was attributed to a dual mechanism which included physical filtration through a microporous structure with pore diameters of 50–200 nm retaining large dye aggregates as well as electrostatic adsorption between the negatively charged membrane surface and the positively charged or cationic MB molecules. The surface charge state was verified by maintaining the pH of the feed solution at its natural value of 6.2 ± 0.3 without adjustment. The silanol groups (Si–OH, pKa ≈ 6.8–7.2) and carboxyl groups (–COOH, pKa ≈

3.1–4.7) were partially deprotonated to form Si–$O^-$ and –$COO^-$ at the pH and the process rendered the membrane surface negatively charged. This facilitated the electrostatic adsorption of cationic MB. The analysis of the permeate solution pH showed an increase to 7.1 ± 0.2 which signaled the release of $H^+$ ions produced by ion exchange during adsorption.

Amino groups (–$NH_2$) introduced through APTES modification further contributed to the process by forming hydrogen bonds with the chromophore groups of MB (Abbas & Shaari, 2025). These results were in line with the observation of Malafatti et al [11] who achieved >90% efficiency with rice husk ash-derived silica membranes and Quellmalz & Mihranyan [3] who reported >95% for citric acid-cross-linked nanocellulose membranes.

**Table 1.** Mechanical properties and separation performance of hybrid paper membranes for all variations (n = 3, mean ± SD)

| Code | Composition (%) | | Membrane Characteristics | | | Membrane Performance | | | |
|---|---|---|---|---|---|---|---|---|---|
| | Silica | Citric Acid | Thickness (µm) | Tensile Strength (MPa) | Strain (%) | Flux (L/m²·h·bar) | Removal Efficiency | | |
| | | | | | | | MB (%) | $Cu^{2+}$ (%) | $Pb^{2+}$ (%) |
| M0 | 0 | 0 | 148 ± 12 | 12.4 ± 1.1 | 8.2 ± 0.9 | 380 ± 18 | 61.2 ± 2.8 | 35.1 ± 4.1 | 38.7 ± 3.9 |
| M1 | 5 | 0 | 156 ± 10 | 14.1 ± 0.8 | 7.6 ± 0.7 | 345 ± 15 | 74.3 ± 3.1 | 48.2 ± 3.5 | 51.6 ± 3.2 |
| M2 | 10 | 0 | 163 ± 90 | 16.8 ± 1.2 | 6.9 ± 0.6 | 318 ± 14 | 82.1 ± 2.4 | 59.4 ± 3.8 | 63.2 ± 3.4 |
| M3 | 15 | 0 | 171 ± 11 | 18.5 ± 0.9 | 6.2 ± 0.8 | 302 ± 12 | 88.5 ± 2.1 | 67.3 ± 3.2 | 70.8 ± 2.9 |
| M4 | 20 | 0 | 168 ± 13 | 17.9 ± 1.1 | 6.5 ± 0.7 | 296 ± 16 | 86.2 ± 2.6 | 64.1 ± 3.7 | 67.5 ± 3.3 |
| M5 | 15 | 5 | 178 ± 80 | 20.1 ± 0.7 | 5.8 ± 0.5 | 292 ± 11 | 91.3 ± 1.8 | 72.5 ± 2.8 | 76.4 ± 2.5 |
| M6 | 15 | 10 | 185 ± 70 | 22.3 ± 0.6 | 5.1 ± 0.4 | 285 ± 10 | >95.0 ± 1.2 | 78.5 ± 3.2 | 82.3 ± 2.8 |
| M7 | 15 | 15 | 182 ± 90 | 21.8 ± 0.8 | 5.4 ± 0.6 | 289 ± 13 | 93.7 ± 1.5 | 76.2 ± 2.9 | 79.8 ± 2.6 |

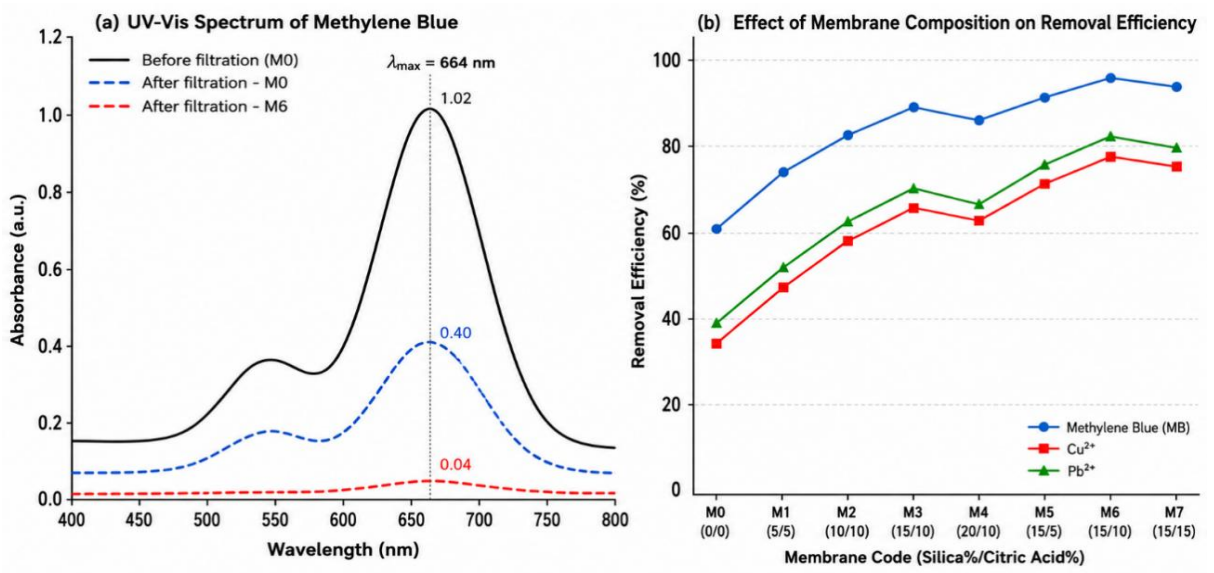


**Figure 1.** (a) UV-Visible spectra of methylene blue (MB) solution before and after filtration with hybrid paper membrane, M0 (0% silica : 0% Citric acid) and M6 (15% silica : 10% citric acid), (b) Plot showing the relationship between membrane composition variations (silica/citric acid) and the removal efficiency of methylene blue (MB), $Cu^{2+}$, and $Pb^{2+}$

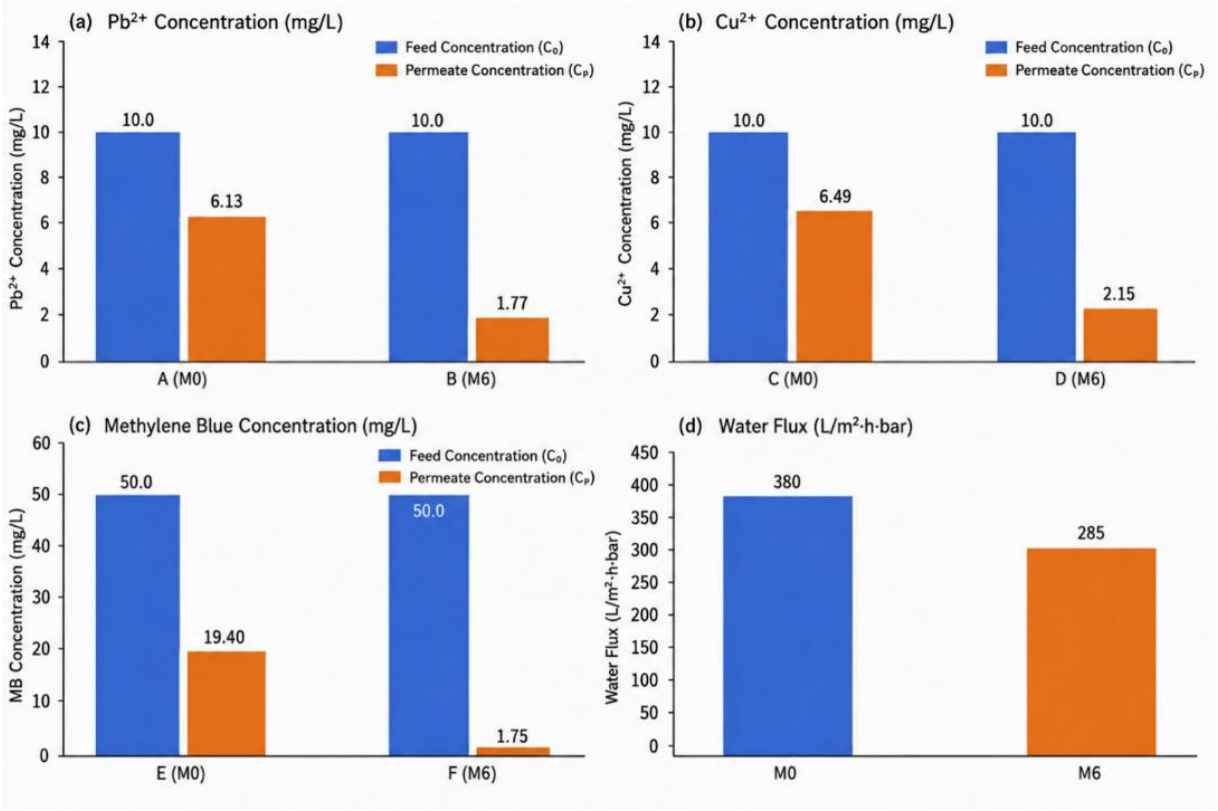


**Figure 2.** Comparison of feed ($C_0$) and permeate ($C_p$) concentrations before and after filtration using M0 (0% silica : 0% Citric acid) and M6 (15% silica : 10% citric acid): (a) $Pb^{2+}$ ions ($C_0$ = 10 mg/L), (b) $Cu^{2+}$ ions ($C_0$ = 10 mg/L), (c) methylene blue (MB) ($C_0$ = 50 mg/L), and (d) water flux (L/m²·h·bar)

$$\text{Membrane–NH}_2 + M^{2+} \rightarrow \text{Membrane–NH}_2\cdots M^{2+} \quad \textbf{(Equation 3)}$$

$$2\ \text{Membrane–COOH} + M^{2+} \rightarrow (\text{Membrane–COO})_2M + 2H^+ \quad \textbf{(Equation 4)}$$

The decrease in flux from 380 L/m²·h·bar in M0 to 285 L/m²·h·bar in M6 reflected an increased flow resistance due to higher pore density and stronger adsorption interactions. However, the flux values were high for laboratory-scale filtration applications. Unmodified pure cellulose membranes typically recorded a water flux of 300–500 L/m²·h·bar [15] while citric acid-cross-linked nanocellulose membranes were reported to show approximately 150–250 L/m²·h·bar at similar pressures [3]. The trend showed that a 25% reduction in flux relative to the control was acceptable because it was offset by an increase in MB removal efficiency from 61% to >95%. The trade-off between flux and selectivity is a common characteristic of filtration membranes and the M6 composition offers the optimal balance.

The results regarding $Cu^{2+}$ and $Pb^{2+}$ heavy metal separation performance present a comparison of the concentrations before and after filtration using M6. Figure 2 is presented as four diagrams including (a) $Pb^{2+}$ ions, (b) $Cu^{2+}$ ions, (c) MB, and (d) the water flux of M0 and M6. Each diagram features a Y-axis that represents concentration units (mg/L) and an X-axis showing conditions before (initial concentration, $C_0$) and after filtration (permeate concentration, $C_p$).

A significant reduction was observed in heavy metal concentration after filtration. M6 achieved a removal efficiency of 78.5 ± 3.2% for $Cu^{2+}$ and 82.3 ± 2.8% for $Pb^{2+}$. M0 recorded only 35.1 ± 4.1% and 38.7 ± 3.9% respectively. The significantly higher reduction observed with M6 reflected that the incorporation of APTES-modified silica and cross-linking with citric acid substantially enhanced the adsorption capacity of the membrane for heavy metal ions. The mechanism of heavy metal ion binding to the membrane requires three primary processes which are complexation with the amino groups (–$NH_2$) from APTES, chelation with the carboxyl groups (–COOH) from citric acid, and ion exchange with the hydroxyl groups (–OH) of the cellulose. The complexation and chelation reactions can be expressed as follows in Equation 3 and 4.

The pH of the heavy metal feed solutions was measured without adjustment at 5.8 ± 0.2 for $Cu^{2+}$ and 5.9 ± 0.2 for $Pb^{2+}$ to ensure that the proposed mechanisms occur under relevant conditions. This range allowed full deprotonation of the –COOH group (pKa ≈ 3.1–4.7) while the $–NH_3^+$ group from APTES (pKa ≈ 9–10) remained in the $–NH_2$ form. The process consequently allowed the membrane surface to possess $–COO^-$ sites for metal chelation and $–NH_2$ sites for complexation. The filtration was followed by the reduction of the permeate pH to 5.1 ± 0.2 to confirm the release of $H^+$ ions in line with the reaction [4].

The slightly higher $Pb^{2+}$ removal efficiency compared to $Cu^{2+}$ can be attributed to differences in ionic characteristics. The $Pb^{2+}$ ion has a larger ionic radius of 1.19 Å than $Cu^{2+}$ with 0.73 Å [16] but has a greater tendency to form complexes with "soft" electron-donor ligands such as amino groups. This is consistent with the Hard and Soft Acids and Bases (HSAB) principle discussed by Lázaro et al [17]. The results were also in line with the report of Natarajan et al [13] who achieved >80% $Pb^{2+}$ removal efficiency using an integral membrane based on rice husk ash silica.

### 3.2 Crystal Structure Analysis Using X-Ray Diffraction (XRD)

XRD characterization was applied to M6 which was classified as the optimal condition based on mechanical test results to show the diffraction pattern at 80°C. The X-axis represents the 2θ angle in degrees and the Y-axis is the intensity. The diffraction patterns (Figure 3) showed semi-crystalline peaks at 2θ angles of approximately 6.83°, 11.49°, and 15.90° as well as dominant peaks at 21.31°, 22.56°, and 23.63°. The peaks in the 2θ range of approximately 21–24° represented the (002) crystallographic plane of the cellulose type I structure. This signaled that the cellulose crystalline framework was preserved after the modification and cross-linking processes [10]. The peak at 15.90° also corresponded to the (101) plane of cellulose type I [18].

The absence of sharp crystalline silica peaks observed typically at 2θ ≈ 26° for crystalline quartz confirmed that the incorporated silica was amorphous and uniformly dispersed within the cellulose matrix. This result was consistent with the observation of Chik et al [4] that rice husk ash silica had a broad amorphous peak at approximately 2θ = 22°. The amorphous structure of silica is advantageous due to the ability to provide a larger specific surface area (≥200 $m^2/g$) and more active sites than crystalline silica which further enhances pollutant adsorption capacity [19].

The crystallinity parameters used for comparison showed that M0 had a sharper cellulose peak with an intensity of 12,847 cps and a crystallinity index (CrI) of 68.4 while M6 recorded a lower peak intensity of 8,923 cps and a reduced CrI of 51.2%. The broadening of the peak at full width at half maximum (FWHM) from 0.92° recorded in M0 to 1.28° for M6 confirmed a decrease in crystalline order. This signaled effective interfacial interaction between the amorphous silica and the cellulose matrix where the presence of dispersed silica particles disrupted the regularity of the cellulose chains.

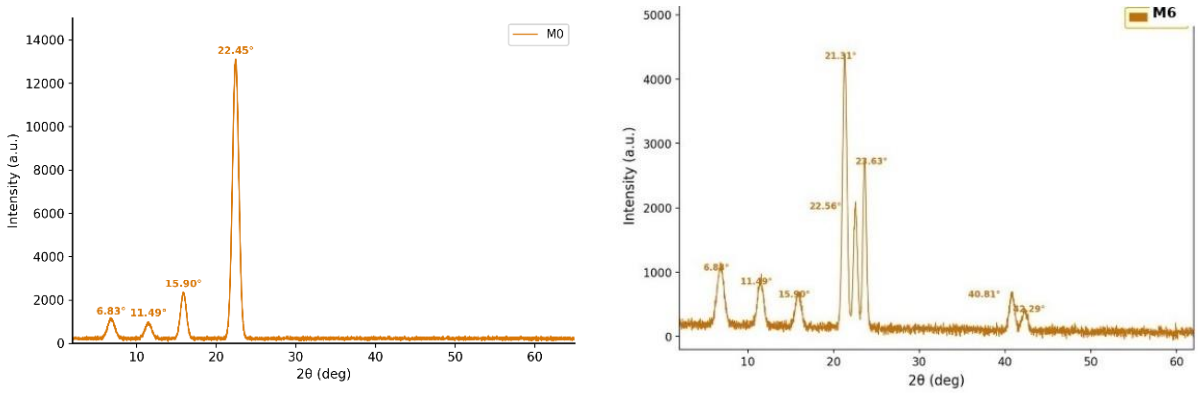


**Figure 3.** X-Ray Diffraction (XRD) patterns of hybrid paper membranes M0 (0% silica : 0% citric acid) and M6 (15% silica : 10% Citric acid) processed at 80°C

### 3.3 Functional Group Analysis Using Fourier-Transform Infrared Spectroscopy (FTIR)

FTIR spectra were recorded for all membrane variations but the results only focused on comparing M0 with M6. The two spectra (Figure 4) were selected to show the most significant changes in functional groups due to the addition of silica and citric acid cross-linking. A comprehensive identification of the functional groups is summarized in the following Table 2.

The absorption band at 1031 $cm^{-1}$ (Si–O–Si) confirmed the successful incorporation of silica into the cellulose matrix. The intensity of this band increased proportionally from M0 (absent) to M6 (highest) in line with the previous reports of Chik et al [4] and Malafatti et al [11]. The band at 1433 $cm^{-1}$ (N–H bending) and at 3300–3500 $cm^{-1}$ (N–H stretching) also confirmed the successful APTES modification of the silica surface [13].

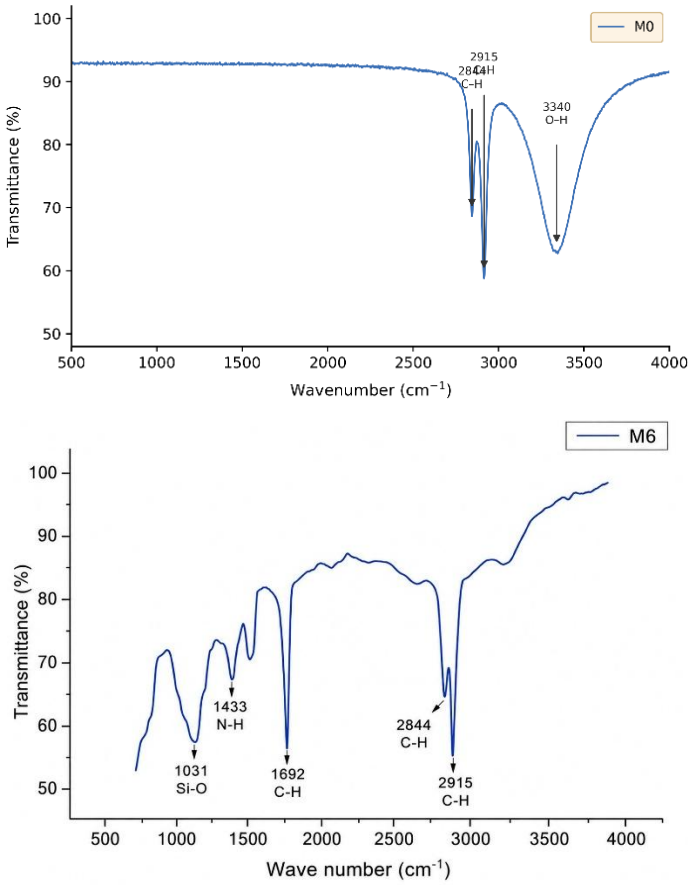


**Figure 4.** Fourier-Transform Infrared Spectroscopy (FTIR) spectra of hybrid paper membranes (0% silica : 0% Citric acid) and M6 (15% silica : 10% citric acid) processed at 80°C

**Table 2.** Identification of functional groups based on FTIR spectra of hybrid paper membranes

| Wavenumber ($cm^{-1}$) | Functional Group | Component | Description |
|---|---|---|---|
| 1031 | Si–O–Si | Silica (rice husk ash) | Silica incorporation confirmed. The intensity increased proportionally with silica content |
| 1433 | N–H bending | Amino group (APTES) | Silica modification successful. N–H stretching also appeared at 3300–3500 $cm^{-1}$ |
| 1692 | C=O carboxyl | Citric acid | Free carboxyl groups from citric acid |
| 1730 | C=O ester | Cross-linking bond | Evidence of ester bonding between citrate –COOH and cellulose –OH appeared after citric acid treatment [13] |
| 2844, 2915 | C–H aliphatic | Cellulose | Cellulose matrix structure preserved after modification |
| 3200–3600 | O–H stretching | Cellulose/water | Hydrophilic nature and intensity decreased after cross-linking |

*The signal at 1730 $cm^{-1}$ shows the peak serving as the primary indicator of successful cross-linking.*

The evidence of ester cross-linking between citric acid and cellulose was reflected through (1) the appearance of a new peak at 1730 $cm^{-1}$ (ester C=O) exclusively in citric acid-treated membranes (M5, M6, M7), and not in those without citric acid (M0–M4). The trend was also observed in (2) a decrease in the intensity of the O–H band at 3200–3600 $cm^{-1}$ due to the consumption of hydroxyl groups during the esterification reaction. These results were consistent with reports by Quellmalz & Mihranyan [3] on cross-linked nanocellulose membranes and Qi et al [20] on cellulose membranes. The band at 1692 $cm^{-1}$ also signaled the presence of C=O groups from the unreacted free carboxyl of citric acid. The simultaneous presence of –OH, $–NH_2$, –COOH, and Si–OH groups provided a multifunctional surface capable of interacting with cationic dyes via electrostatic forces and heavy metal ions through complexation and chelation [10],[21].

### 3.4 Surface Morphology Analysis Using Scanning Electron Microscopy (SEM)

Figure 5 shows SEM images of hybrid paper membranes M0 and M6 at 20,000× magnification based on the method proposed by Malafatti et al [11]. The purpose was to observe the distribution of silica particles on the membrane surface. A non-homogeneous surface morphology featuring irregularly sized particle aggregates attached to the fiber matrix as well as a porous structure with micropores ranging from 50 to 200 nm in diameter was observed. The elemental composition was subsequently confirmed through the application of Energy-Dispersive Spectroscopy (EDS) on M6 and M0 with the results presented in Table 3.

The relatively uniform distribution of silica represented by the low standard deviation for Si (±0.5%), suggested that the APTES modification successfully enhanced compatibility between the silica and the cellulose matrix. This was achieved through the interactions between amino groups ($–NH_2$) and cellulose hydroxyl groups (–OH) to form strong interfacial hydrogen bonds [4],[13]. The porous structure which featured micropores sized 50–200 nm facilitated physical filtration of large particles such as dye aggregates while dissolved pollutants in the form of heavy metal ions and dye molecules interacted with active adsorption sites on the pore walls [12],[22]. This morphology was similar to the report of Hubadillah et al [12] on rice husk ash-based hollow fiber ceramic membranes used for heavy metal removal. The trend was also similar to the observation of Stamina et al [2] regarding the cellulose acetate membranes derived from rice husk waste.

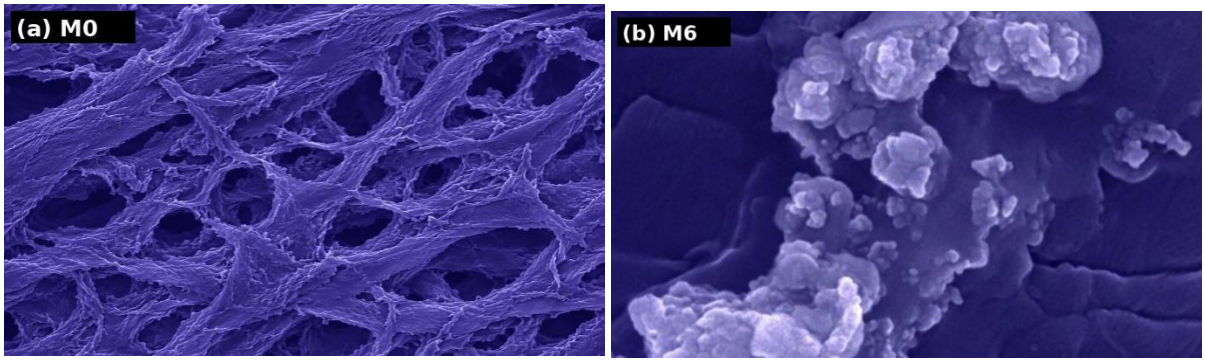


**Figure 5.** Scanning Electron Microscopy (SEM) images of hybrid paper membranes (0% silica : 0% Citric acid) and M6 (15% silica : 10% citric acid) at 20,000× magnification

**Table 3.** Elemental composition from Energy-Dispersive Spectroscopy (EDS) analysis for (0% silica : 0% Citric acid) and M6 (15% silica : 10% citric acid)

| Element | M0 (Control) | M6 (Optimal) | Description |
|---|---|---|---|
| **C (at.%)** | 58.3 ± 2.1 | 47.6 ± 1.8 | Derived from a cellulose matrix |
| **O (at.%)** | 40.1 ± 1.9 | 42.7 ± 1.6 | Derived from cellulose and silica |
| **Si (at.%)** | 0.0 ± 0.0 | 8.2 ± 0.5 | Evidence of silica incorporation (M6 only) |
| **N (at.%)** | 0.0 ± 0.0 | 1.2 ± 0.3 | Derived from APTES amino groups (M6 only) |
| **Na (at.%)** | 1.6 ± 0.4 | 0.3 ± 0.1 | Residue from the extraction process (negligible) |

*Values are expressed as the mean ± standard deviation from three measurement points in different areas. The elements Si and N were detected only in M6 to confirm the successful incorporation of APTES-modified silica.*

3.5 Membrane Regeneration and Reusability Tests

As shown in the Table 4, the removal efficiency for MB remained above 85% and the values for $Cu^{2+}$ and $Pb^{2+}$ were higher than 70% and 75% respectively after three cycles. The performance decline of approximately 7–10% per cycle was possibly attributable to the accumulation of incompletely desorbed pollutants and slight damage to the pore structure caused by acid treatment. However, M6 showed promising regeneration potential for repeated use which was comparable to other reported cellulose-based membranes [2].

3.6 Statistical Analysis and Composition Optimization

A two-way ANOVA was conducted at a 95% confidence level ($\alpha = 0.05$) to evaluate the effects of silica content, citric acid concentration, and the interaction on pollutant removal efficiency. The analysis covered the removal efficiency for MB, $Cu^{2+}$, and $Pb^{2+}$.

The ANOVA results showed that silica content ($p < 0.001$), citric acid concentration ($p < 0.001$), and their interaction ($p < 0.05$ for all pollutants) significantly affected the removal efficiency of MB, $Cu^{2+}$, and $Pb^{2+}$. The significant interaction was a sign that the effect of adding silica was not independent of the citric acid concentration and vice versa.

A Tukey HSD post-hoc test was conducted to compare differences between pairs of membrane compositions. Table 6 presents the post-hoc test results for MB removal efficiency as a representative example and similar results were obtained for $Cu^{2+}$ and $Pb^{2+}$.

**Table 4.** Removal efficiency of the membrane M6 over three regeneration cycles (n=3, mean ± SD)

| Cycle | MB Removal Efficiency (%) | $Cu^{2+}$ Removal Efficiency (%) | $Pb^{2+}$ Removal Efficiency (%) |
|---|---|---|---|
| **1** | 95.2 ± 1.1 | 78.8 ± 3.0 | 82.5 ± 2.7 |
| **2** | 91.5 ± 1.4 | 74.2 ± 3.5 | 78.9 ± 3.1 |
| **3** | 88.3 ± 1.6 | 70.5 ± 3.8 | 75.6 ± 3.4 |

**Table 5.** Two-way ANOVA results for removal efficiency (n = 3 with degrees of freedom = 1 for each main factor and 1 for the interaction)

| Source of Variation | DF | MB | $Cu^{2+}$ | $Pb^{2+}$ | | | |
|---|---|---|---|---|---|---|---|
| | | F | p-value | F | p-value | F | p-value |
| **Silica Content** | 1 | 124.56 | <0.001 | 98.34 | <0.001 | 105.78 | <0.001 |
| **Citric Acid Concentration** | 1 | 87.23 | <0.001 | 72.16 | <0.001 | 79.45 | <0.001 |
| **Interaction (Silica × Citric Acid)** | 1 | 5.89 | 0.023 | 6.12 | 0.019 | 5.97 | 0.021 |
| **Residual** | 20 | | | | | | |

*DF = degrees of freedom; F = calculated F-value; p-value = significance (p < 0.05 = significant effect). F-values were calculated using SPSS 25.0.*

**Table 6.** Tukey HSD post-hoc test results for methylene blue (MB) removal efficiency across membrane compositions ($\alpha = 0.05$)

| Membrane Code | M0 | M1 | M2 | M3 | M4 | M5 | M6 | M7 |
|---|---|---|---|---|---|---|---|---|
| **M0 (0/0)** | - | 0.012* | 0.003* | 0.001* | 0.001* | 0.001* | 0.001* | 0.001* |
| **M1 (5/0)** | 0.012* | - | 0.041* | 0.008* | 0.010* | 0.002* | 0.001* | 0.003* |
| **M2 (10/0)** | 0.003* | 0.041* | - | 0.032* | 0.045* | 0.018* | 0.001* | 0.021* |
| **M3 (15/0)** | 0.001* | 0.008* | 0.032* | - | 0.079 | 0.042* | 0.001* | 0.038* |
| **M4 (20/0)** | 0.001* | 0.010* | 0.045* | 0.079 | - | 0.038* | 0.001* | 0.042* |
| **M5 (15/5)** | 0.001* | 0.002* | 0.018* | 0.042* | 0.038* | - | 0.002* | 0.136 |
| **M6 (15/10)** | 0.001* | 0.001* | 0.001* | 0.001* | 0.001* | 0.002* | - | 0.001* |
| **M7 (15/15)** | 0.001* | 0.003* | 0.021* | 0.038* | 0.042* | 0.136 | 0.001* | - |

*Values listed are p-values. The asterisk (*) indicates a significant difference at α = 0.05. Composition code: (silica%/citric acid%). M6 (15/10) differs significantly from all other membranes (p < 0.05).*

Table 6 shows that M6 has MB removal performance considered statistically significantly different ($p < 0.05$) from all other variations ranging from M0 through M5 and M7. The same trend applies to the removal efficiency of $Cu^{2+}$ and $Pb^{2+}$. An increase in the silica content from 15% to 20% which focused on comparing M3 vs. M4 did not significantly improve efficiency ($p = 0.079 > 0.05$ for MB; $p > 0.05$ for heavy metals). Similarly, a rise in the citric acid content from 10% to 15% (M6 vs. M7) did not produce a significant difference ($p = 0.136$ for MB). This showed that the optimum composition was 15% silica and 10% citric acid (M6). Any increase in the content above these values tended to cause silica particle agglomeration and an excess of unbound carboxyl groups which caused the inability to significantly improve performance [3].

## 4. Conclusion

In conclusion, this research successfully developed a hybrid paper membrane based on abaca fibers from Ogan Ilir, South Sumatra and rice husk ash silica using citric acid as a cross-linking agent for the removal of the dye MB and heavy metal ions $Cu^{2+}$ and $Pb^{2+}$ from synthetic wastewater. Amorphous silica was successfully extracted from rice husk ash with >90% efficiency and modified using APTES. This modification was confirmed by the appearance of amino groups in the FTIR spectrum at 1433 $cm^{-1}$ and 3300–3500 $cm^{-1}$. The formation of ester cross-links between citric acid and cellulose was evidenced by a new peak at ~1730 $cm^{-1}$ (ester C=O) and a decrease in O–H intensity in the citric acid-treated membranes. Moreover, SEM analysis reported a uniform silica distribution at a Si content of 8.2 ± 0.5% with micropores sized 50–200 nm which facilitated the mechanisms of both physical filtration and simultaneous adsorption.

The optimal membrane which was designated M6 and contained 15% silica and 10% citric acid had the best performance including a removal efficiency of >95% for MB, 78.5 ± 3.2% for $Cu^{2+}$, and 82.3 ± 2.8% for $Pb^{2+}$ in addition to a water flux of 285 $L/m^2 \cdot h \cdot bar$ at 1 bar pressure. The two-way ANOVA results also confirmed that silica content, citric acid concentration, and their interaction significantly affected separation performance ($p < 0.05$). Future research should investigate membrane durability and regenerability through cyclic testing, optimize pH and contact time, and evaluate performance at a pilot-plant scale using actual industrial wastewater to validate the potential for commercial application.

**AI Usage Statements**

During the preparation of this manuscript, the authors used Grammarly (Grammarly Inc.), ChatGPT (GPT-4, OpenAI), and Claude (Anthropic) for language polishing, literature search assistance, paraphrasing, and structural editing. All AI-generated outputs were critically reviewed and thoroughly edited by the authors to ensure factual accuracy, clarity of expression, and compliance with academic standards. The authors take full responsibility for the integrity and content of this manuscript.

**CRediT Authorship Statement**

**Ian Kurniawan:** Conceptualization, Methodology, Writing, Original Draft, Supervision, Project administration. **Adri Huda:** Formal analysis, Data curation, Validation. **Reisya Ichwani:** Investigation, Resources, Software. **Dina Nasution**: Visualization, Writing, Review & Editing. **Nasrul Rofiah Hidayati**: Methodology, Validation, Formal analysis. **Noor Haida Mohd Kaus:** Supervision, Writing Review & Editing, Funding acquisition.

**Declaration of competing interest**

The authors declare there are no conflict of interests. The authors declare that they have no known competing financial interests or personal relationships that could have appeared to influence the work reported in this paper.

## References

[1] Astuti, W., & Susilowati, N. (2014). Sintesis adsorben berbasis Lignoselulosa dari kayu randu (Ceiba pentandral.) Untuk menjerap Pb (II) dalam Limbah cair artifisial. *Jurnal Bahan Alam Terbarukan*, 3(2), 50-54.

[2] Stamina, N., Hashim, N. A., Ong, L. De, Rabuni, M. F., & Abdul Manaf, N. (2024). Unlocking the potentialities of biomass-based cellulose acetate membrane from waste rice husk for water treatment. *Chemical Papers*, 78(10), 5793-5804.

[3] Quellmalz, A., & Mihranyan, A. (2015). Citric acid cross-linked nanocellulose-based paper for size-exclusion nanofiltration. *ACS Biomaterials Science & Engineering*, 1(4), 271-276.

[4] Chik, N. S. I., & Shaari, N. Z. K. (2023). Integral Membrane Properties of Polysulfone/Chitosan/Polyvinyl Alcohol Blend Incorporated with Rice Husk Ash Silica Gel. *Indonesian Journal of Chemistry*, 23(3).
[5] Environesia Global Saraya. (2025, juliol 9). Limbah Industri dan Ancaman Pencemaran Air di Indonesia. *Environesia*.
[6] Kurniawan, I., Rahman, D. Y., Hanafi, F., Rahman, M. I., Suryana, A. T., Lestari, A., … Huda, A. (2026). High stability and performance of organic pollutant removal using PVDF-TiO. *Journal of Ecological Engineering*, 27(5), 430-443.
[7] Liu, H., Pan, Y., Jin, S., Sun, X., Jiang, Y., Wang, Y., … Cui, Q. (2021). Associations between six common per-and polyfluoroalkyl substances and estrogens in neonates of China. *Journal of Hazardous Materials*, 407, 124378.
[8] Sapei, L., Padmawijaya, K. S., Sutejo, A., & Theresia, L. (2015). Karakterisasi silika sekam padi dengan variasi temperatur leaching menggunakan asam asetat. *Jurnal Teknik Kimia*, 9(2), 38-43.
[9] Gastaldon, F., Junca, E., Grillo, F. F., Sobieranski, A. C., Gomes, S. Q., Rafique, J., … Frizon, T. E. A. (2025). Cellulosic membranes supported with silica from rice husk and rice husk ash for slow release. *Química Nova*, 48(4), e-20250095.
[10] Zainuddin, N. A. F. M., Shaari, N. Z. K., Chik, N. S. I., & Hamzah, F. (2023). Evaluation of crosslinking degree on the integral membrane by using Rice Husk Ash (RHA). *Journal of Mechanical Engineering (JMechE)*, 20(2), 57-71.
[11] Malafatti, J. O. D., Tavares, F. A., Neves, T. R., Mascarenhas, B. C., Quaranta, S., & Paris, E. C. (2023). Modified silica nanoparticles from rice husk supported on polylactic acid as adsorptive membranes for dye removal. *Materials*, 16(6), 2429.
[12] Hubadillah, S. K., Othman, M. H. D., Tai, Z. S., Jamalludin, M. R., Yusuf, N. K., Ahmad, A., … Harun, Z. (2020). Novel hydroxyapatite-based bio-ceramic hollow fiber membrane derived from waste cow bone for textile wastewater treatment. *Chemical Engineering Journal*, 379, 122396.
[13] Natarajan, E., Markandan, K., Hassan, C. S. B., & Koppad, P. G. (2017). Sustainable Structural Materials.
[14] Bindir, H. S., Ahmed, R. A., Bello, A., Sanni, S. E., Ngene, P., Fashedemi, O. O., … Onwualu, A. P. (2025). Experimental determination of the mechanical and hydrolytic properties of chitosan/rice husk ash composite membranes. *International Journal of Biological Macromolecules*, 286, 138390.
[15] Mautner, A., & Bismarck, A. (2021). Bacterial nanocellulose papers with high porosity for optimized permeance and rejection of nm-sized pollutants. *Carbohydrate polymers*, 251, 117130.
[16] Hawthorne, F. C., & Gagné, O. C. (2024). New ion radii for oxides and oxysalts, fluorides, chlorides and nitrides. *Structural Science*, 80(4), 326-339.
[17] Lázaro, I.A., Chen, X., Ding, M., Eskandari, A., Fairen-Jimenez, D., Giménez-Marqués, M., … Forgan, R. S. (2024). Metal–organic frameworks for biological applications. *Nature Reviews Methods Primers*, 4(1), 42.
[18] Raja, P. M., Rangkuti, I. U. P., Hendra Ginting, M., Giyanto, & Siregar, W. F. (2021). Preparation and characterization of cellulose microcrystalline made from palm oil midrib. En *IOP Conference Series: Earth and Environmental Science* (Vol. 819, p. 012002). IOP Publishing.
[19] Phanthong, P., Reubroycharoen, P., Hao, X., Xu, G., Abudula, A., & Guan, G. (2018). Nanocellulose: Extraction and application. *Carbon Resources Conversion*, 1(1), 32-43.
[20] Qi, F., Qi, B., Cui, Z., Chen, X., Wan, Y., & Luo, J. (2025). Cellulose-based separation membranes: A sustainable evolution or fleeting trend? *Advanced Membranes*, 5, 100153. doi: https://doi.org/10.1016/j.advmem.2025.100153
[21] Huong, T. T., & Trang, T. Y. D. (2023). Removal of lead ions from aqueous media using rice husk modified with manganese oxide. *Environ. Ecol. Res*, 11(2), 340-361.
[22] Tran, N.-A., Hien, N. T., Hoang, N. M., Dang, H.-L. T., Huy, D. Q., Van Quy, T., … Dao, V.-D. (2023). Carbon dots in environmental treatment and protection applications. *Desalination*, 548, 116285.